ISSN 0025-6544, Mechanics of Solids, 2010, Vol. 45, No. 3, pp. 370–378. © Allerton Press, Inc., 2010.
Original Russian Text © A.M. Krivtsov, E.A. Podol'skaya, 2010, published in Izvestiya Akademii Nauk. Mekhanika Tverdogo Tela, 2010, No. 3, pp. 77–86.

Modeling of Elastic Properties of Crystals with Hexagonal Close-Packed Lattice

A. M. Krivtsov* **and E. A. Podol'skaya****

Institute for Problems in Mechanical Engineering, Russian Academy of Sciences, Bol'shoy pr-t 61, St. Petersburg, 199178 Russia

Received January 30, 2010

Abstract—In the present paper, we consider mechanical properties of an ideal hexagonal close-packed (HCP) crystal lattice. We construct three models for describing the elastic characteristics of metals with HCP lattice. Using examples of nine metals with different degree of geometric imperfection (beryllium, hafnium, cadmium, cobalt, magnesium, rhenium, titanium, zinc, and zirconium), we show that including the moment interaction into the model leads to a more accurate description of the elastic properties than taking into account the geometric features of a specific lattice. We also show that, depending on the type of the electron shell, it is efficient to use different models; namely, for d-elements, it suffices to use the two-parameter force model, while for the s-elements, it is required to take the moment interaction into account.

DOI: 10.3103/S0025654410030076

Key words: *HCP lattice, elastic properties, moment interaction, electron shell, bulk compression modulus.*

1. INTRODUCTION

Recently, the particle dynamics method [1–3], in which the material is represented as a set of points particles or rigid bodies moving according to the laws of classical mechanics, became especially topical because of the necessity to describe the mechanical processes at the nanometer scale level [4–10]. In this case, the particle dynamics method is very important not only as a computational method but also as a powerful analytical tool for investigating the material behavior at the nanolevel and for establishing the relationship between the material micro- and macroparameters [1,11–15].

In nanotechnologies, it is required to determine the mechanical properties of objects whose dimensions are commensurable with interatomic distances, and hence the specific characteristics of their atomic structure must be taken into account explicitly. Many nanostructures are either ideal crystals or contain significant monocrystal segments, and hence it is necessary to develop the mathematical apparatus and mechanical models of crystal solid deformation for obtaining a correct description of nanoobjects and for their exploitation [16–18]. Moreover, the possibility to relate the micro- and macroparameters is important for stating the problems of computer simulation.

In the present paper, we consider the analytical modeling of one of the most widely used crystal structures: the hexagonal close-packed (HCP) lattice. An anisotropic potential based on the Morse potential, which takes the interatomic bond direction into account, was proposed in [17]. The bonds in the first six coordination spheres were taken into account. This potential ensures stability and reflects the symmetry of hexagonal crystal lattices, but the computations of elastic moduli by using this potential do not give correct results for all metals. Moreover, since the lattice symmetry is explicitly taken into account, it is impossible to use such a potential in the case of large strains and structural transitions. In the present paper, we propose to consider only the first coordination sphere, which significantly simplifies the calculations and is sufficient for describing the elastic properties (also without transition to large strains).

*e-mail: akrivtsov@bk.ru, anton.m.krivtsov@gmail.com
**e-mail: katepodolskaya@gmail.com

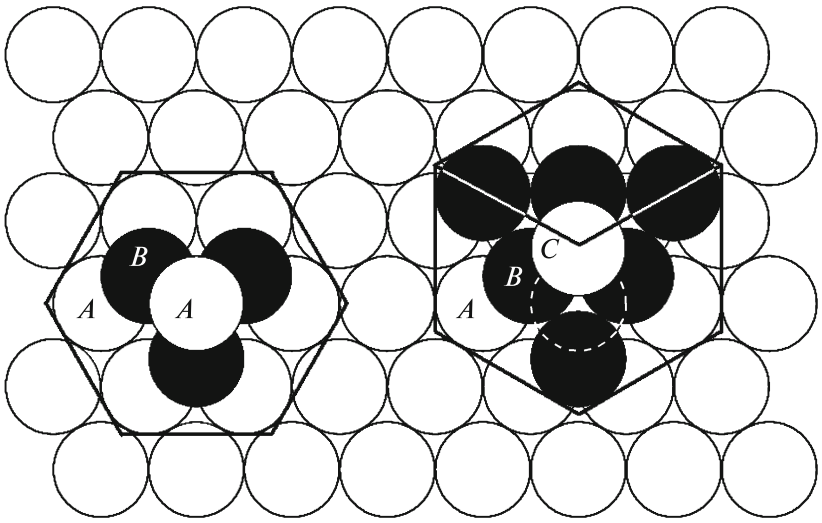

Fig. 1.

Close-packed lattices are lattices in which the maximal concentration of nodes per unit volume is attained for a given minimal distance between the nodes. Such a structure can be visually represented by rigid balls arranged into layers in a certain volume (Fig. 1). In contrast to directed bonding in covalent crystals, bonding in metal crystals is spherically symmetric [19]. Therefore, in crystallography, an actual metal atom is replaced by a rigid ball whose radius, the so-called metallic radius of an atom, is equal to half the distance between the nearest neighboring atoms. The following two closely packed structures are encounter most often. In crystallography, they are called the face-centered cubic (FCC) and hexagonal close-packed (HCP) lattices [19]. The difference between the FCC (to the right) and HCP (to the left) lattices can be seen in Fig. 1.

The HCP lattice has a two-layer periodicity and the sequence of its layers is written in the form $\ldots ABABAB \ldots$; the FCC lattice is a three-layer periodicity characterized by the sequence $\ldots ABCABC \ldots$. The packing density, which is the ratio of the total volume occupied by the balls per cell to the total volume of the cell, is the same for both lattices, but they have significant topological distinctions. The FCC lattice is simple: all atoms (and A and B and C) are in the same position with respect to their environment. The HCP lattice is more complicated—it is diatomic; with respect to the atoms in even (B) and odd (A) layers, the surrounding atoms are located differently. Conditionally, we say that the atoms in adjacent layers (A and B) are atoms of different type, although the atoms themselves are the same, and only the environment geometry is different. Any complicated lattice can be represented as several simple sublattices embedded into one another. The HCP lattice has two such sublattices; they can be obtained as the union of respective even and odd atomic layers. In contrast to the FCC lattice, the HCP lattice has no cubic symmetry. The importance of taking account of two atoms in an elementary cell of the HCP lattice was investigated, for example, in [20] when developing an X-ray method for studying the short-range order in polycrystal HCP alloys.

Moreover, in actual crystals the distances between neighboring atoms belonging to the same or different layers are always the same for the FCC lattice (this follows from the cubic symmetry). For the HCP lattice, these distances differ to a lesser or greater extent, so that the actual HCP lattice corresponds to the close packing of ellipsoids rather than balls. The lattice of actual metals is said to be geometrically imperfect. In closely packed structures, each atom obviously has 12 nearest neighbors, which are called the first coordination sphere. In the lattice of actual metals, these 12 neighbors cannot be called the first coordination sphere, because 6 of them are closer to the central (reference) atom than the others. Nevertheless, to avoid confusion in considering many coordination spheres, to the first coordination sphere in a geometrically imperfect lattice, we ascribe the atoms that would belong to it if it were a perfect lattice.

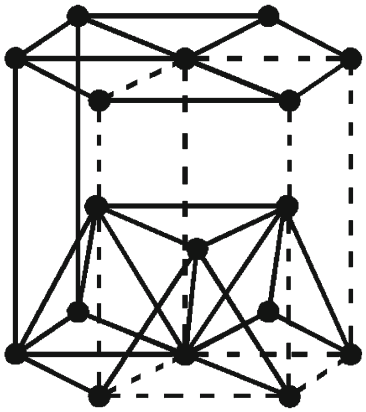

Fig. 2.

2. MODELING TECHNIQUES. BASIC RELATIONS

The models are constructed by the particle dynamics method according to which the material (a continuous medium) can be represented as a set of particles or rigid bodies mutually interacting by certain laws. By doing so, one passes from a continuous model to a discrete model, which is one of the most important steps on the way from microworld to macroworld. An important problem is to obtain relations between macroscopic and microscopic elastic characteristics, namely, between the components of the lattice stiffness tensor and the interparticle bonding stiffnesses. In the present paper, we construct two "force" and one "moment" models.

The models are constructed using direct tensor calculus [21, 22]. The vector quantities are denoted by lowercase boldface characters (e.g., $\mathbf{a}$ and $\mathbf{b}$) and the tensor quantities, by uppercase boldface characters (e.g., $\mathbf{A}$ and $\mathbf{B}$). The rank of a tensor is denoted by a left superscript; for example, ${}^3\mathbf{C}$ is a tensor of rank 3. For tensors of rank 2, this superscript will be usually omitted. A tensor of rank n is a sum of terms each of which is the tensor product of n vectors. The tensor product is associative and distributive in both vectors and scalar number, but it is not commutative: vectors in the tensor product cannot be permuted.

The force model is based on the idea that separate particles forming the lattice interact through a pair potential depending only on the distance between the particles (for example, the Lenard–Jones or Morse potential), but the form of the potential is not specified. In the first approximation, each particle (atom, lattice node) turns out to be connected with its 12 nearest neighbors that form the first coordination sphere by linear springs whose spring constants (stiffnesses) will be called microscopic. For a closely packed lattice, such a model, based only on the central interaction, is stable. The stiffness tensor of a complicated diatomic lattice in the case of force interaction can be calculated by the formulas [1]:

$$ {}^4\mathbf{C} = {}^4\mathbf{C}_* - {}^3\mathbf{C} \cdot {}^2\mathbf{C}^{-1} \cdot {}^3\mathbf{C}, \tag{2.1} $$

$$ {}^2\mathbf{C} = \frac{1}{V_0}\sum_\alpha \nu_\alpha c_\alpha \mathbf{n}_\alpha \mathbf{n}_\alpha, \quad {}^3\mathbf{C} = \frac{1}{V_0}\sum_\alpha \nu_\alpha a_\alpha c_\alpha \mathbf{n}_\alpha \mathbf{n}_\alpha \mathbf{n}_\alpha, \quad {}^4\mathbf{C}_* = \frac{1}{V_0}\sum_\alpha a_\alpha^2 c_\alpha \mathbf{n}_\alpha \mathbf{n}_\alpha \mathbf{n}_\alpha \mathbf{n}_\alpha, \tag{2.2} $$

where $\mathbf{n}_\alpha$ are unit vectors of bond directions, a_α and c_α are the bond lengths and stiffnesses, $\nu_\alpha = 0$ for the interaction of atoms of the same type, $\nu_\alpha = 1$ for the interaction of atoms of different types, and V_0 is the volume of the elementary cell. For the HCP lattice, this is a right prism whose base is a rhombus with angle 60° (dashed lines in Fig. 2). The summation is performed over all atoms interacting with the reference atom. The type of the reference atom is of no importance.

Formulas (2.1) and (2.2) were obtained under the assumption that, in equilibrium, the interaction forces between the atoms of the crystal are zero (or negligibly small). The deformation of a complicated lattice consists of the deformation of sublattices and their mutual displacement. The tensor ${}^4\mathbf{C}^*$ characterizes the crystal elastic stiffness without taking account of the sublattice displacements; the tensor ${}^2\mathbf{C}$ characterizes the stiffness with respect to the sublattice displacements; and the tensor ${}^3\mathbf{C}$ describes the mutual influence of the two types of deformation.

In a description that uses moment (noncentral) interaction, rods with longitudinal and transverse stiffnesses are introduced instead of springs. For the case of moment interaction, the following formulas

for the stiffness tensors of a diatomic lattice were obtained in [23]:

$$
\begin{aligned}
&{}^2\mathbf{C} = \frac{1}{V_0}\sum_\alpha \nu_\alpha[(c_A - c_D)\mathbf{n}_\alpha\mathbf{n}_\alpha + c_D\mathbf{E}], \quad {}^3\mathbf{C} = \frac{c_A - c_D}{V_0}\sum_\alpha \nu_\alpha a_\alpha \mathbf{n}_\alpha\mathbf{n}_\alpha\mathbf{n}_\alpha,\\
&{}^4\mathbf{C}_* = \frac{1}{V_0}\sum_\alpha [(c_A - c_D)a_\alpha^2\mathbf{n}_\alpha\mathbf{n}_\alpha\mathbf{n}_\alpha\mathbf{n}_\alpha + c_D\mathbf{n}_\alpha\mathbf{E}\mathbf{n}_\alpha]^S,
\end{aligned}
\tag{2.3}
$$

where c_A and c_D are the longitudinal and transverse stiffnesses of the bond and $\mathbf{E}$ is the unit tensor of rank 2. The symbol S denotes the symmetry with respect to all the vectors contained in the tensor product.

3. ONE-PARAMETER FORCE MODEL

We consider the simplest model of ideal HCP lattice, namely, the model in which the distance between any atom and all its neighbors in the first coordination sphere is the same as well as the stiffness of their bonds. Such a model is one-parameter, because it contains a single microscopic elastic characteristic.

For the HCP lattice, we assume that $\nu_\alpha = 0$ in the case of interaction of the nearest neighbors in one layer ($\alpha = 1, \ldots, 6$) and $\nu_\alpha = 1$ in the case of interaction of the nearest neighbors in adjacent layers (for $\alpha = 7, \ldots, 12$).

Then formulas (2.2) take the form

$${}^2\mathbf{C} = \frac{c}{V_0}\sum_{\alpha=7}^{12}\mathbf{n}_\alpha\mathbf{n}_\alpha, \quad {}^3\mathbf{C} = \frac{ca}{V_0}\sum_{\alpha=7}^{12}\mathbf{n}_\alpha\mathbf{n}_\alpha\mathbf{n}_\alpha, \quad {}^4\mathbf{C}_* = \frac{ca^2}{V_0}\sum_{\alpha=1}^{12}\mathbf{n}_\alpha\mathbf{n}_\alpha\mathbf{n}_\alpha\mathbf{n}_\alpha, \quad V_0 = \sqrt{2}a^3, \tag{3.1}$$

where a and c are the bond length and stiffness.

We introduce an orthonormal basis $\mathbf{i}, \mathbf{j}, \mathbf{k}$ so that the vectors $\mathbf{i}$ and $\mathbf{j}$ lies in the atomic layer plane and the vector $\mathbf{k}$ is perpendicular to the layer.

Then the vectors $\mathbf{n}_\alpha$ can be represented as

$$\mathbf{n}_{1,4} = \pm\mathbf{i}, \quad \mathbf{n}_{8,11} = \frac{\sqrt{3}}{3}\mathbf{j} \pm \frac{\sqrt{3}}{6}\mathbf{k}, \quad \mathbf{n}_{2,3,5,6} = \pm\frac{1}{2}\mathbf{i} \pm \frac{\sqrt{3}}{2}\mathbf{j}, \quad \mathbf{n}_{7,9,10,12} = \pm\frac{1}{2}\mathbf{i} - \frac{\sqrt{3}}{6}\mathbf{j} \pm \frac{\sqrt{6}}{3}\mathbf{k}. \tag{3.2}$$

Substituting these expressions into formulas (3.1), we obtain

$$
\begin{aligned}
&{}^2\mathbf{C} = \frac{c}{V_0}(\tilde{\mathbf{E}} + 4\mathbf{k}\mathbf{k}), \quad {}^3\mathbf{C} = \frac{\sqrt{3}}{6}\frac{ca^3}{V_0}\mathbf{J}, \quad {}^4\mathbf{C}_* = \frac{ca^2}{V_0}\left[\frac{5}{2}(\tilde{\mathbf{E}}\tilde{\mathbf{E}})^S + 4(\tilde{\mathbf{E}}\mathbf{k}\mathbf{k})^S + \frac{8}{3}\mathbf{k}\mathbf{k}\mathbf{k}\mathbf{k}\right],\\
&\tilde{\mathbf{E}} = \mathbf{i}\mathbf{i} + \mathbf{j}\mathbf{j}, \quad {}^3\mathbf{J} = \mathbf{j}\mathbf{j}\mathbf{j} - 3(\mathbf{i}\mathbf{i}\mathbf{j})^S.
\end{aligned}
\tag{3.3}
$$

The symbol S denotes the symmetrization with respect to all vectors contained in the tensor product, in particular,

$$
\begin{aligned}
&(\mathbf{i}\mathbf{i}\mathbf{j})^S = \tfrac{1}{3}(\mathbf{i}\mathbf{i}\mathbf{j} + \mathbf{i}\mathbf{j}\mathbf{i} + \mathbf{j}\mathbf{i}\mathbf{i}), \quad (\tilde{\mathbf{E}}\tilde{\mathbf{E}})^S = \tfrac{1}{3}(\tilde{\mathbf{J}}_1 + \tilde{\mathbf{J}}_{23}), \quad \tilde{\mathbf{J}}_1 = \tilde{\mathbf{E}}\tilde{\mathbf{E}},\\
&\tilde{\mathbf{J}}_{23} = 2\mathbf{i}\mathbf{i}\mathbf{i}\mathbf{i} + 2\mathbf{j}\mathbf{j}\mathbf{j}\mathbf{j} + \mathbf{i}\mathbf{j}\mathbf{j}\mathbf{i} + \mathbf{j}\mathbf{i}\mathbf{i}\mathbf{j} + \mathbf{i}\mathbf{j}\mathbf{i}\mathbf{j} + \mathbf{j}\mathbf{i}\mathbf{j}\mathbf{i},\\
&(\tilde{\mathbf{E}}\mathbf{k}\mathbf{k})^S = \tfrac{1}{6}(\tilde{\mathbf{E}}\mathbf{k}\mathbf{k} + \mathbf{k}\tilde{\mathbf{E}}\mathbf{k} + \mathbf{k}\mathbf{k}\tilde{\mathbf{E}} + \mathbf{i}\mathbf{k}\mathbf{i}\mathbf{k} + \mathbf{j}\mathbf{k}\mathbf{j}\mathbf{k} + \mathbf{k}\mathbf{i}\mathbf{k}\mathbf{i} + \mathbf{k}\mathbf{j}\mathbf{k}\mathbf{j} + \mathbf{i}\mathbf{k}\mathbf{k}\mathbf{i} + \mathbf{j}\mathbf{k}\mathbf{k}\mathbf{j}).
\end{aligned}
\tag{3.4}
$$

It follows from the geometric considerations that the stiffness tensor ${}^4\mathbf{C}_*$ given by formula (3.3) is the stiffness tensor of the FCC lattice under the nearest neighbor interaction. The second term in (2.1) can be calculated as

$${}^3\mathbf{C}\cdot{}^2\mathbf{C}^{-1}\cdot{}^3\mathbf{C} = \frac{1}{12}\frac{ca^2}{V_0}{}^3\mathbf{J}\cdot{}^3\mathbf{J} = \frac{1}{12}\frac{ca^2}{V_0}(\tilde{\mathbf{J}}_{23} - \tilde{\mathbf{J}}_1). \tag{3.5}$$

Then, according to (2.1), for the stiffness tensor of the HCP lattice, we obtain

$${}^4\mathbf{C} = \frac{ca^2}{V_0}\left[\frac{11}{12}\tilde{\mathbf{J}}_1 + \frac{3}{4}\tilde{\mathbf{J}}_{23} + 4(\tilde{\mathbf{E}}\mathbf{k}\mathbf{k})^S + \frac{8}{3}\mathbf{k}\mathbf{k}\mathbf{k}\mathbf{k}\right]. \tag{3.6}$$

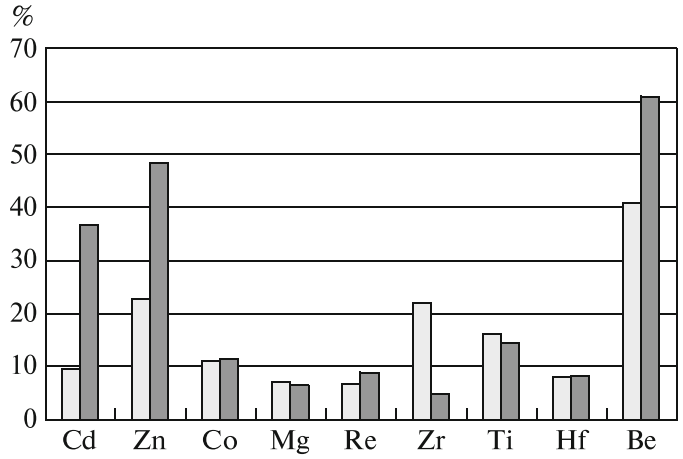

Fig. 3.

From (3.6) we derive the analytic expressions for the stiffness tensor components (in the three-dimensional case, a 6×6 matrix corresponds to it) in terms of the bond stiffness and length:

$$C_{11} = C_{22} = \frac{29\sqrt{2}}{24}\frac{c}{a}, \quad C_{33} = \frac{4\sqrt{2}}{3}\frac{c}{a}, \quad C_{12} = \frac{11\sqrt{2}}{24}\frac{c}{a},$$
$$C_{13} = C_{23} = C_{44} = C_{55} = \frac{\sqrt{2}}{3}\frac{c}{a}, \quad C_{66} = \frac{3\sqrt{2}}{8}\frac{c}{a}. \tag{3.7}$$

Here $C_{2323} = C_{44}$, $C_{3131} = C_{55}$, and $C_{1212} = C_{66}$.

The other components can be obtained from the above expressions by permutations of indices, for example, $C_{21} = C_{12}$. The bulk compression modulus is determined by the formula

$$K^{(1)} = \frac{1}{9}\mathbf{E} \cdot\cdot\, {}^4\mathbf{C} \cdot\cdot\, \mathbf{E} = \frac{2\sqrt{2}}{3}\frac{c}{a}. \tag{3.8}$$

Further, the bond stiffness c for several HCP metals (beryllium, hafnium, cadmium, cobalt, magnesium, rhenium, titanium, zinc, zirconium) was calculated on the basis of experimental data [17] for the stiffness tensor component C_{11} and the bond length a. Also the following verification was performed: two experimental values of the bulk modulus K and $\tilde{K}$ [17, 24] were compared with the bulk modulus $K^{(1)}$ calculated by formula (3.8). Since the difference between K and $\tilde{K}$ was less than 20%, a result was regarded as satisfactory if it differed from both values by no more than 20%. This criterion is satisfied for metals whose bond lengths are approximately the same in all directions (Fig. 3). In Fig. 3, the light-shaded regions show the deviation $|K^{(1)} - K|/K$, and the dark-shaded regions show the deviation $|K^{(1)} - \tilde{K}|/\tilde{K}$.

4. TWO-PARAMETER FORCE MODEL

Now we consider the model that takes account of the lattice geometric imperfection for different metals, where the interatomic distance within the same layer differs from that for adjacent layers. So we consider two bond lengths and, accordingly, two bond stiffnesses, and the model thus becomes two-parameter. Just as in the case of the one-parameter force model, we obtain the following expressions for the components of the stiffness tensor and the bulk compression modulus:

$$C_{11} = \frac{\sqrt{3}}{3a_0\eta}\left(\frac{9}{2}c_0 + \frac{4}{4+3\eta^2}c\right), \quad C_{13} = C_{55} = \frac{2\sqrt{3}\eta c}{a_0(4+3\eta^2)}, \quad C_{12} = \frac{\sqrt{3}}{3a_0\eta}\left(\frac{3}{2}c_0 + \frac{4}{4+3\eta^2}c\right),$$
$$C_{33} = \frac{3\sqrt{3}\eta^3 c}{a_0(4+3\eta^2)}, \quad K^{(2)} = \frac{\sqrt{3}}{9a_0\eta}\left(4c_0 + \frac{4+3\eta^2}{3}c\right), \quad C_{66} = \frac{\sqrt{3}c_0}{2a_0\eta}, \tag{4.1}$$

where a_0 and c_0 are the length and stiffness of the bond between neighboring atoms lying in the same layer, a and c is the length and stiffness of the bond between neighboring atoms lying in adjacent layers,

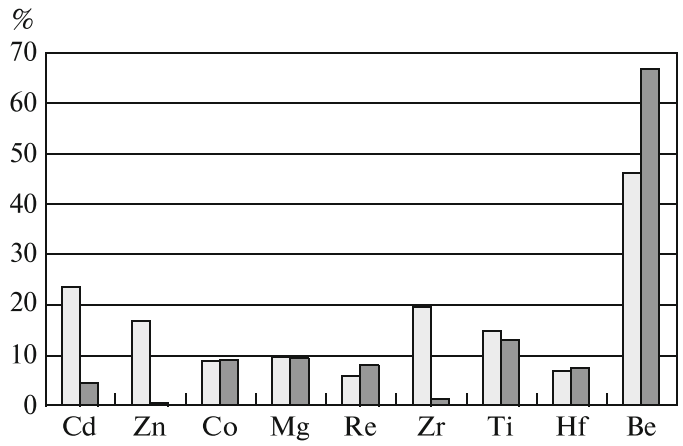

Fig. 4.

$\eta = 2h/a_0$, and $h = \sqrt{a^2 - a_0^2/3}$ is the distance between neighboring layers (in the case of ideal geometry, $\eta = \eta_0 = 2\sqrt{2/3}$).

Further, on the basis of experimental data [17] for the stiffness tensor components C_{11} and C_{33} and the bond length a_0, the bond stiffnesses c_0 and c were calculated and then the bulk compression moduli were compared (Fig. 4). In Fig. 4, the light-shaded regions show the relative deviation $|K^{(2)} - K|/K$, and the dark-shaded regions show $|K^{(2)} - \tilde{K}|/\tilde{K}$. Here K and $\tilde{K}$ are the experimental values [17, 24] and $K^{(2)}$ is determined by (4.1).

It turned out that, taking the geometric imperfection into account enabled to decrease the difference between the experimental and computational values of this modulus, especially for metals whose bond lengths in different directions differ by 13–15% (zinc, cadmium). When analyzing the two force models, it was noted that the bond stiffness decreases as the bond length increases.

Beryllium was the only exception among metals under study, for which the results predicted by the two force models give a discrepancy that is 2–3 times larger than the adopted allowed value. It is well known that most of the above-considered HCP metals are d-elements, in which both the outermost and the previous electronic subshells participate in the interatomic interaction. But beryllium has only two electronic subshells and is an s-element.

5. MOMENT MODEL

Now we consider the moment model of an ideal HCP lattice. It is also a two-parameter lattice, we introduce rods with both the tensile and bending stiffnesses instead of springs.

We use formulas (2.1) and (2.3) to calculate the stiffness tensor components

$$C_{11} = \frac{\sqrt{2}}{4a}\left[5c_A + 3c_D - \frac{(c_A - c_D)^2}{6(c_A + 5c_D)}\right], \quad C_{13} = \frac{\sqrt{2}}{3a}(c_A - c_D),$$
$$C_{12} = \frac{\sqrt{2}(c_A - c_D)(11c_A + 49c_D)}{24a(c_A + 5c_D)}, \quad C_{33} = \frac{2\sqrt{2}}{3a}(2c_A + c_D), \tag{5.1}$$
$$C_{66} = \frac{\sqrt{2}}{12a}\left[5c_A + 7c_D - \frac{(c_A - c_D)^2}{2(c_A + 5c_D)}\right], \quad C_{44} = \frac{\sqrt{2}}{3a}(c_A + 2c_D), \quad K^{(3)} = \frac{2\sqrt{2}}{3a}c_A,$$

where c_A and c_D are the bond longitudinal and transverse stiffnesses and a is the bond length.

Comparison with experimental data shows that the moment model works better than the one-parameters model for all metals and better than the two-parameter model for all metals except zinc and cadmium, whose geometric imperfection is too strong (Fig. 5). In Fig. 5, the light-shaded regions show the relative deviation $|K^{(3)} - K|/K$, the dark-shaded regions represent $|K^{(3)} - \tilde{K}|/\tilde{K}$. Here K and $\tilde{K}$ are experimental values [17, 24], and $K^{(3)}$ is determined by formula (5.1).

An important result is that this model can describe beryllium.

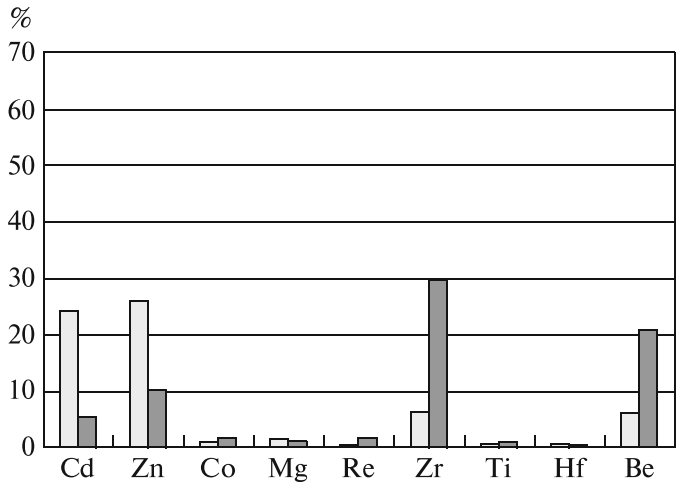

Fig. 5.

Table 1

	Metal (group, subgroup)	ζ, %	$c^{(1)}$, N/m	$c_0^{(2)}$, N/m	$c^{(2)}/c_0^{(2)}$	c_A, N/m	c_D/c_A
I	Cd (II B)	15.49	12.6	15.4	0.262	8.7	−0.893
	Zn (II B)	13.67	15.7	18.9	0.232	9.5	−0.863
II	Co (VIII B)	−0.006	28.2	28.1	1.062	31.3	−0.096
	Mg (II A)	−0.55	7.0	7.0	0.946	7.4	−0.243
	Re (VII B)	−1.11	61.8	60.8	1.045	66.7	−0.129
III	Zr (IV B)	−2.48	16.9	16.3	1.127	23.1	−0.476
	Ti (IV B)	−2.72	17.5	16.9	1.096	20.8	−0.298
	Hf (IV B)	−3.06	21.1	20.3	1.081	23.2	−0.207
	Be (II A)	−3.25	24.4	23.2	1.156	18.4	0.766

6. RESULTS AND CONCLUSIONS

Table 1 presents the computational results for several HCP metals. We introduce the notation: $\zeta = (\eta - \eta_0)/\eta_0$ is the dimensionless parameter characterizing the lattice geometry (for a geometrically perfect lattice, we have $\zeta = 0$), $c^{(1)}$ is the interatomic bond stiffness calculated on the basis of the one-parameter model, $c_0^{(2)}$ and $c^{(2)}$ are the respective bond stiffnesses in the layer plane and between the layers (the two-parameter force model), and c_A and c_D are the respective longitudinal and transverse bond stiffnesses (the moment model). All the stiffnesses were determined on the basis of experimental data for C_{11} and C_{33} with the well-known dimensions of the elementary cell taken into account [17, 24].

Depending on the value of the parameter ζ, the above-considered metals can be divided into three groups, denoted by the Roman numerals I, II, and III in the table. For the first group (Cd and Zn), we have the inequality $\zeta > 0$ (the lattice is elongated along the vertical axis of symmetry), and the stiffness of the bond issuing from the plane is approximately four times less than that of the bond lying in the plane. For the second group (Mg, Co, and Re), we can assume that $\zeta \approx 0$, and the difference between $c^{(2)}$ and $c_0^{(2)}$ is approximately 5%. For the third group (Zr, Ti, and Hf), we have $\zeta < 0$ (the lattice is compressed along the vertical axis of symmetry), and the difference between $c^{(2)}$ and $c_0^{(2)}$ increases up to 8–16%.

In the moment model for all the above-considered metals except for beryllium, the transverse bond stiffness is, first, less than the longitudinal bond stiffness and, second, negative. Thus, the introduction of the moment interaction slightly destabilized the lattice (although the stability was not lost) in order to, apparently, compensate the geometric imperfection, which was not taken into account. The fact that c_D

is negative can testify that the metallic bond is nondirectional. In the case of beryllium, the transverse bond stiffness is positive.

Thus, we can conclude that (i) in the majority of cases, a correct choice of the interaction is more important than taking account of the geometric characteristics of a specific lattice and (ii) the choice of the interaction depends on the type of the metal electronic subshell; in particular, *d*-elements can be described with a sufficient accuracy by purely force models.

ACKNOWLEDGMENTS

The research was financially supported by the Grant of the Saint-Petersburg Government (decision No. 68 taken on June 20, 2008) and by the Russian Foundation for Basic Research (projects Nos. 08-01-00865-a and 09-01-12096-ofi-m).

REFERENCES

1. A. M. Krivtsov, *Deformation and Failure of Solids with Microstructure* (Fizmatlit, Moscow, 2007) [in Russian].
2. R. W. Hockney and J. W. Eastwood, *Computer Simulation Using Particles* (A. Hilger, New York, 1988).
3. M. P. Allen and A. K. Tildesley, *Computer Simulation of Liquids* (Clarendon Press, Oxford, 1987).
4. R. V. Goldstein and A. V. Chentsov, "Discrete–Continuous Model of a Nanotube," Izv. Akad. Nauk. Mekh. Tverd. Tela, No. 4, 57–74 (2005) [Mech. Solids (Engl. Transl.) **40** (4), 45–59 (2005)].
5. R. V. Goldstein, V. A. Gorodtsov, and D. S. Lisovenko, "Mesomechanics of Multilayer Carbon Nanotubes and Nanowhiskers," Fizich. Mezomekh. **11** (6), 25–42 (2008).
6. A. M. Krivtsov and N. F. Morozov, "Anomalies in Mechanical Characteristics of Nanometer-Size Objects," Dokl. Ross. Akad. Nauk **381** (3), 345–347 (2001) [Dokl. Phys. (Engl. Transl.) **46** (11), 825–827 (2001)].
7. E. A. Gudilin, A. V. Garshev, A. E. Baranchikov, et al., *The Riches of the Nanoworld. Photo Reportage from the Depths of Matter*, Ed. by Yu. D. Tret'yakov (BINOM, Laboratoriya Znanii, Moscow, 2009) [in Russian].
8. A. Yu. Kuksin, G. E. Norman, V. V. Stegailov, and A. V. Yanilkin, "Molecular Simulation as a Scientific Base of Nanotechnologies in Power Engineering," J. Engng Thermophys. **18** (3), 197–226 (2009).
9. B. D. Annin, S. N. Korobeynikov, and A. V. Babichev, "Computer Simulation of a Twisted Nanotube Buckling," Sib. Zh. Industr. Mat. **11** (1), 3–22 (2008) [J. Appl. Industr. Math. (Engl. Transl.) **3** (3), 318–333 (2009)].
10. Ch. P. Poole, Jr., and F. J. Owens, *Nanotechnologies*, 4th ed. revised and completed (Wiley, New York, 2003; Tekhnosfera, Moscow, 2009).
11. A. M. Krivtsov, *Elastic Properties of One-Atomic and Two-Atomic Crystals* (Izd. Politekh. Univ., St. Petersburg, 2009) [in Russian].
12. I. E. Berinskii, N. G. Dvas, A. M. Krivtsov, et al. *Theoretical Mechanics. Elastic Properties of One-Atomic and Two-Atomic Crystals*, Ed. by A. M. Krivtsov, (Izd-vo Politekh. Univ., St. Petersburg, 2009) [in Russian].
13. Y. Chen, "Local Stress and Heat Flux in Atomistic Systems Involving Three-Body Forces," J. Chem. Phys. **124**, 054113 (2006).
14. J. A. Zimmerman, R. E. Jones, and J. A. Templeton, "A Material Frame Approach for Evaluating Continuum Variables in Atomistic Simulations," J. Comp. Phys. **229** (1), 2364–2389 (2010).
15. V. M. Fomin, I. F. Golovnev, and A. V. Utkin, "Relation between the Atomic Picture and Continuum Mechanics Description of Detonating Solid-State Explosives," Shock Waves **13** (1), 155–165 (2003).
16. E. A. Ivanova, A. M. Krivtsov, N. F. Morozov, and A. D. Firsov, "Description of Crystal Packing of Particles with Torque Interaction," Izv. Akad. Nauk. Mekh. Tverd. Tela, No. 4, 110–127 (2003) [Mech. Solids (Engl. Transl.) **38** (4), 76-88 (2003)].
17. N. A. Baranov, E. A. Dubov, I. V. Dyatlova, and E. V. Chernykh, "Atomic-Discrete Description of the Effect of Anisotropic Interatomic Interactions on the Elastic Properties of Metals with a Hexagonal Close-Packed Lattice," Fiz. Tverd. Tela **46** (2), 212–217 (2004) [Phys. Solid State (Engl. Transl.) **46** (2), 213–218 (2004)].
18. E. I. Golovneva, I. F. Golovnev, and V. M. Fomin, "Modeling of Quasistatic Processes in Crystals by a Method of Molecular Dynamics," Fizich. Mezomekh. **6** (6), 5–10 (2003).
19. D. M. Vasil'ev, *Physical Crystallography* (Metallurgiya, Moscow, 1981) [in Russian].
20. V. M. Silonov, E. V. Evlyukhina, O. V. Kris'ko, and A. B. Evlyukhin, "Influence of Interatomic Correlation Effects on Short-Range Order in Hexagonal Close-Packed Polycrystalline Alloys," Fiz. Tverd. Tela **41** (12), 2009–2015 (1999) [Phys. Solid State (Engl. Transl.) **41** (12), 1933–1939 (1999)].
21. P. A. Zhilin, *Vectors and Tensors of Rank Two in Three-Dimensional Space* (Nestor, St. Petersburg, 2001) [in Russian].

22. A. I. Lurie, *Nonlinear Theory of Elasticity* (Nauka, Moscow, 1980) [in Russian].
23. E. A. Ivanova, A. M. Krivtsov, and N. F. Morozov, "Derivation of Macroscopic Relations of the Elasticity of Complex Crystal Lattices Taking into Account the Moment Interactions at the Microlevel," Prikl. Mat. Mekh. **71** (4), 595–615 (2007) [J. Appl. Math. Mech. (Engl. Transl.) **71** (4), 543–561 (2007)].
24. I. S. Grigoriev and E. Z. Meilikhov (Editors), *Physical Quantities, Reference Book* (Energoatomizdat, Moscow, 1991) [in Russian].